[redacted]

Copy 207
RM L53L08a

[redacted]

NACA RM L53L08a

7509

TECH LIBRARY KAFB, NM
01h4286

NACA

RESEARCH MEMORANDUM

EXPERIMENTAL CONVECTIVE HEAT TRANSFER TO A 4-INCH AND 6-INCH HEMISPHERE AT MACH NUMBERS FROM 1.62 TO 3.04

By Leo T. Chauvin and Joseph P. Maloney

Langley Aeronautical Laboratory
Langley Field, Va.

CLASSIFIED DOCUMENT

[redacted]

NATIONAL ADVISORY COMMITTEE
FOR AERONAUTICS

WASHINGTON
February 3, 1954

[redacted]

[redacted]

Classification cancelled (or changed to Unclassified)

By Authority of NASA Tech Pub Announcement

(OFFICER AUTHORIZED TO CHANGE)

92 15 Nov 55

By .....

.....

(GRADE OF OFFICER MAKING CHANGE)

10 Apr 61

DATE

TECH LIBRARY KAFB, NM
0144286

N

NACA RM L53L08a

[redacted]

NATIONAL ADVISORY COMMITTEE FOR AERONAUTICS

RESEARCH MEMORANDUM

EXPERIMENTAL CONVECTIVE HEAT TRANSFER TO A 4-INCH AND 6-INCH HEMISPHERE AT MACH NUMBERS FROM 1.62 TO 3.04

By Leo T. Chauvin and Joseph P. Maloney

SUMMARY

Experimental investigation of supersonic aerodynamic heat transfer has been conducted on hemispheres. The manner in which heat-transfer coefficient varies along a spherical surface has been determined for a Mach number range from 1.62 to 3.04. The variation of equilibrium temperatures along the surface was also determined. Although heat-transfer coefficients and equilibrium temperatures were found to be independent of Mach number over the range tested, heat-transfer coefficients were found to vary 14 percent for a change in the ratio of surface temperature to adiabatic wall temperature from 0.70 to 0.96. Transition from a laminar to a turbulent boundary layer was obtained at a Reynolds number (based on length along the surface from the stagnation point) of approximately 1×10^6, corresponding to a region on the body located between the 45° and 60° stations. Comparison of the heat transfer at the stagnation point with theory is presented and shows good agreement.

INTRODUCTION

From the standpoint of minimum drag, high fineness ratio and nearly pointed noses are desirable in the design of supersonic missiles and airplanes. However, it is necessary for some supersonic vehicles to have hemispherical noses to house guidance equipment. The use of this nose shape may result in severe drag penalties and high skin temperatures. Reference 1 presents the results of a previous investigation on aerodynamic heat transfer to a hemisphere at $M = 2.8$. However, the model used was influenced by large magnitude of heat conduction. The National Advisory Committee for Aeronautics has made tests in the preflight jet of the Langley Pilotless Aircraft Research Station at Wallops Island, Va. to determine the pressure drag, pressure distribution, and aerodynamic heating of hemispherical noses. The pressure distribution and pressure drag for a

[redacted]

[redacted]

hemispherical nose at $M = 2.05$, 2.54, and 3.04 have been reported in reference 2. The test results presented herein are for the aerodynamic heating on a hemispherical nose 4 inches in diameter at Mach numbers of 1.62 to 3.04 and for a Reynolds number of approximately 4.5×10^6 based on nose diameter. Additional tests were made at $M = 1.99$ on a hemispherical nose 6 inches in diameter. Reynolds number for this test was approximately 6.4×10^6, and tests were made for two different degrees of surface smoothness. These Reynolds numbers for both models were based on properties of the air in the undisturbed free stream.

SYMBOLS

M	Mach number
V	velocity, ft/sec
h	local heat-transfer coefficient, Btu/(sec)(sq ft)($^\circ$F)
T_w	skin temperature, $^\circ$R
T_e	equilibrium skin temperature, $^\circ$R
T_s	stream stagnation temperature, $^\circ$R
T_{aw}	adiabatic wall temperature, $^\circ$R
τ	skin thickness, ft
c	specific heat of skin, Btu/lb $^\circ$F
d	mass density of wall, lb/cu ft
t	time, sec
l	length along the surface from the stagnation point on the model, ft
ρ	density of air, slugs/cu ft
μ	absolute viscosity of air, lb-sec/sq ft
c_p	specific heat of air at constant pressure, Btu/slug $^\circ$F
k	thermal conductivity of air, Btu/(sec)(ft)($^\circ$F)

[redacted]

[redacted]

Nu	Nusselt number,	$h\ell/k$
Pr	Prandtl number,	$c_p\mu/k$
R	Reynolds number,	$\rho V\ell/\mu$
C_H	Stanton number,	$\frac{h}{\rho c_p V} = \frac{Nu}{Pr\ R}$

APPARATUS, MODELS, AND TESTS

The 4-Inch Model

The preflight jet test facility is a blowdown-type tunnel, supplying air from storage spheres to an 8-inch auxiliary jet and a 12-inch main jet. The 4-inch model was tested in the 8-inch auxiliary jet which utilized interchangeable nozzles to obtain different Mach numbers. Reference 2 showed that the flow properties along the hemisphere was not influenced by the relatively large ratio of model diameter to jet diameter. Elaboration on the details of the preflight jet test facility can be secured from reference 3.

Steady flow conditions are obtained approximately 5 to 8 seconds after initial opening of the jet exhaust valve. In order to prevent the model from being subjected to any jet starting transients, the model was inserted into the air stream after steady flow was established. Inserting the model was accomplished by mounting the model support on a pivoted strut which was swung into the flow by a quick-operating hydraulic system. Prior to each test the model was clear of the air stream and then was injected into test position in 0.5 second. A position indicator recorded the model location as it moved into the flow. All the test results are for the model alined with the center line of the jet. A photograph of the model and strut in the test position is shown in figure 1.

The 4-inch-diameter model was a hemispherical nose, made of K-monel, 0.037-inch thick, and having a smooth and highly polished surface.

Eight no. 36 iron-constantan thermocouples were fused to the inner surface of the hemispherical nose. Stagnation temperatures were measured ahead of the nozzle throat and at the model support.

All measurements were recorded on recording galvanometers, synchronized by means of a timer having a frequency of 10 cycles per second. The instruments were accurate to 1 percent of their full-scale deflections which corresponds to $\pm 5^\circ$ F.

[redacted]

The Reynolds number for the test Mach numbers of 1.62, 2.05, 2.54, and 3.04 were 3.80×10^6, 4.54×10^6, 4.86×10^6, and 3.93×10^6, respectively, based on body diameter and free-stream conditions. The small change in Reynolds number with Mach number was due to the variation in static pressure and temperature. The tests at $M = 1.62$ and 2.05 were for approximately sea-level conditions, whereas the tests at $M = 2.54$ and 3.04 were for a static pressure corresponding to an altitude of approximately 13,000 and 28,000 feet, respectively. Testing at steady flow conditions was maintained until several seconds after equilibrium conditions had been established. The air supply was sufficient to enable testing at the desired flow conditions for approximately 55 seconds.

The 6-Inch Model

The 6-inch-diameter model was tested in the 12-inch main jet of the preflight test facility. The tests were made in a two-dimensional nozzle. A photograph of the model mounted in the jet is shown in figure 2.

The model was made of 0.057-inch-thick K-monel. Two tests were conducted on this model, the first with a smooth and highly polished surface and the second with a roughened surface. The roughened surface corresponded to a light sand blast.

Nine iron-constantan thermocouples were installed on the inner surface of the model. Thermocouple locations for both hemispheres can be obtained from figure 3. The model was mounted on a fixed support and unlike the 4-inch model was subjected to heating during the starting of the jet. The stagnation temperature measured in the heat exchanger, total pressure, and skin temperature measurements were recorded on recording galvanometers.

The Mach number for both the smooth and roughened models was 1.99 and the Reynolds number based on body diameter was 6.4×10^6 which corresponds to sea-level conditions. Steady flow was maintained for 50 seconds, at which time the skin temperatures were essentially in equilibrium.

RESULTS AND DISCUSSION

Equilibrium Temperatures

The measured equilibrium temperatures for the 4-inch and 6-inch noses are shown in figure 3. The values were obtained at approximately 50 seconds after the start of the test when it was observed that the skin had reached a thermal equilibrium. The equilibrium skin temperature expressed

as a ratio to stagnation temperature is plotted on a radial scale which indicates the location at which the measurements were made. The measurements from the 4-inch nose show a temperature ratio of 1 corresponding to stagnation temperature occurring at the front of the nose. The equilibrium temperature decreases gradually along the surface and at the 90° station the skin temperature is about 95 percent of the stagnation temperature.

Equilibrium temperatures are not shown for the stagnation point and the 12° station on the 6-inch nose because of thermocouple failure. Thermocouples at the stagnation point and at the 70° station on the rough nose also malfunctioned.

Data for the test at $M = 3.04$ on the 4-inch nose were confined to the stations from 30° forward because the low static pressures in the nozzle caused a normal shock whose influence was felt beyond the 45° station, as shown in reference 2.

Heat-Transfer Coefficient

The aerodynamic heat-transfer coefficient was measured during the transient heating of the model after the establishment of steady air flow from the nozzle. Radiation from the model and conduction along the surface were calculated and found to be negligible. By neglecting these terms, the convective heat transferred to the model can be equated to the heat absorbed by the model skin per unit of time.

$$h(T_{aw} - T_w) = \tau c d \, dT_w/dt$$

The heat-transfer coefficient h can then be obtained from this equation.

For conditions where radiation and conduction are negligible, the measured equilibrium skin temperature T_e is equal to the adiabatic wall temperature T_{aw}.

The aerodynamic heat-transfer coefficients were evaluated by this equation, taking the mass density of the K monel skin as 555 lb/cu ft and its specific heat as 0.127 Btu/lb/°F. The skin temperature and its time rate of change were obtained from the measured time histories of the skin temperature. The adiabatic wall temperatures were computed from the experimentally determined temperature ratio T_e/T_s. A typical skin temperature and stagnation temperature variation with time is shown in figure 4.

Measured aerodynamic heat-transfer data are presented in figure 5 as Stanton number plotted against Reynolds number for various heating conditions. The heating condition, expressed as a ratio of wall temperature to adiabatic wall temperature, varied from 0.70 to 0.96 during the experimental investigation. The air properties in the Stanton and Reynolds numbers obtained from reference 4 are based on conditions just outside the boundary layer, and the length term in Reynolds number is taken as the distance along the surface from the stagnation point to the measurement station. Local conditions outside the boundary layer were calculated by assuming isentropic flow behind the nose shock and by utilizing reference 2 for the static pressures on the body. Heat-transfer data are shown for the 4-inch- and 6-inch-diameter hemispheres having smooth and highly polished surfaces for Mach numbers from 1.62 to 3.04, and for the 6-inch-diameter hemisphere having a rough surface at a Mach number of 1.99.

Data points for the 4-inch nose are shown in figures 5(a), (b), (c), and (d) for temperature ratios T_w/T_{aw} equal to 0.70, 0.80, 0.90, and 0.96, respectively. The 6-inch-nose data points were confined to a temperature ratio of 0.96 only (fig. 5(d)) since the data at lower temperature ratios were obtained during the period of unsteady flow associated with starting the jet.

Laminar flow prevailed on the 4-inch nose for Reynolds numbers to approximately 1×10^6, corresponding to approximately the 45° station. Beyond the 45° station the data dispersed from the trend established during the laminar region; this dispersion indicates the flow was undergoing transition to turbulence. During this transition, a large increase in heat transfer is effected by small changes in Reynolds number. Consequently, the equilibrium temperatures for stations beyond 45° in figure 3 are characteristic of transitional and turbulent flow. Heat transfer for fully developed turbulent flow is shown in figure 5(d) for the roughened 6-inch hemisphere having a temperature ratio of 0.96.

The heating-condition effect on the laminar heat transfer is demonstrated by plotting the lines representing the faired data from each of the four heating conditions on a composite curve (fig. 5(e)). As the heating condition T_w/T_{aw} increased, the Stanton number, which contains the heat-transfer coefficient, decreases proportionately. These faired curves yielded the following empirical equation for the laminar heat transfer on a hemispherical surface.

$$C_H = 1.46\ R^{-0.556}\left(\frac{T_w}{T_{aw}}\right)^{-0.5}$$

For an increase in T_w/T_{aw} from 0.70 to 0.96 a decrease of 14 percent occurred in C_H.

Since the data presented in each of the heating conditions investigated covered a range of Mach numbers from 1.62 to 3.04, the lack of any systematic scatter of the data points indicated that no Mach number effect was present in this range. This laminar heat transfer was not unexpected, however, as the stations in the laminar flow region were also in the region of subsonic flow behind the bow wave.

Figure 6(a) presents the heat-transfer data measured at the stagnation point on the 4-inch hemispherical nose. The data are plotted according to a theory presented in reference 5 which correlates the stagnation-point heat transfer as $Nu\ Pr^{-0.4} = 1.32R^{0.5}$. The flow conditions are based on the air properties just behind the center of the bow wave, and the length parameter is the diameter of the body. The discrepancy between theory and experiment is partially due to the fact that heating effect is not accounted for in the equation, whereas the data show a trend with heating condition. The experimental data are for a range of heating T_w/T_{aw} from 0.7 to 0.9. Figure 6(b) gives the comparison between the calculated time histories of skin temperature using the theory of reference 5 for the heat-transfer coefficient and the measured skin temperature to $M = 2.05$. The maximum deviation of the theoretical skin temperature from the measured skin temperature was approximately 20° F. Similar agreement was obtained for other Mach numbers investigated.

CONCLUDING REMARKS

Equilibrium skin temperatures and convective heat transfer have been measured on a 4-inch- and 6-inch-diameter hemispherical nose. The Mach number for the 4-inch nose ranged from 1.62 to 3.04 for a Reynolds number based on body diameter of approximately 4.5×10^6. The 6-inch nose was tested at $M = 1.99$ at a Reynolds number based on body diameter of 6.4×10^6 and for two surface conditions.

The measured equilibrium skin temperature for these tests was equal to the stagnation temperature at the 0° station (stagnation point) and decreased gradually along the surface to 95 percent of the stagnation temperature at the 90° station.

Transition from a laminar to a turbulent boundary layer occurred on the hemisphere at a Reynolds number of about 1×10^6 corresponding to a region between the 45° and 60° station.

The heat-transfer data indicated the influence of the heating condition expressed as the ratio of the wall temperature to the adiabatic wall temperature T_w/T_{aw} from 0.70 to 0.96. An increase in heat transfer

was noted at the onset of transition on the smooth nose, approaching the turbulent values measured on a roughened nose.

Heat transfer was measured at the stagnation point which when compared with theory yielded good agreement.

Langley Aeronautical Laboratory,
National Advisory Committee for Aeronautics,
Langley Field, Va., November 24, 1953.

REFERENCES

1. Korobkin, Irving: Local Flow Conditions, Recovery Factors and Heat-Transfer Coefficients on the Nose of a Hemisphere-Cylinder at a Mach Number of 2.8. NAVORD Rep. 2865 (Aeroballistic Res. Rep. 175), U. S. Naval Ord. Lab. (White Oak, Md.), May 5, 1953.

2. Chauvin, Leo T.: Pressure Distribution and Pressure Drag for a Hemispherical Nose at Mach Numbers 2.05, 2.54 and 3.04. NACA RM L52K06, 1952.

3. O'Sullivan, William J., Chauvin, Leo T., and Rumsey, Charles B.: Exploratory Investigation of Transpiration Cooling To Alleviate Aerodynamic Heating on an 8° Cone in a Free Jet at a Mach Number of 2.05. NACA RM L53H06, 1953.

4. Keenan, Joseph H., and Kaye, Joseph: Thermodynamic Properties of Air Including Polytropic Functions. John Wiley & Sons, Inc., 1945.

5. Sibulkin, M.: Heat Transfer Near the Forward Stagnation Point of a Body of Revolution. Jour. Aero. Sci. (Readers' Forum), vol. 19, no. 8, Aug. 1952, pp. 570-571.

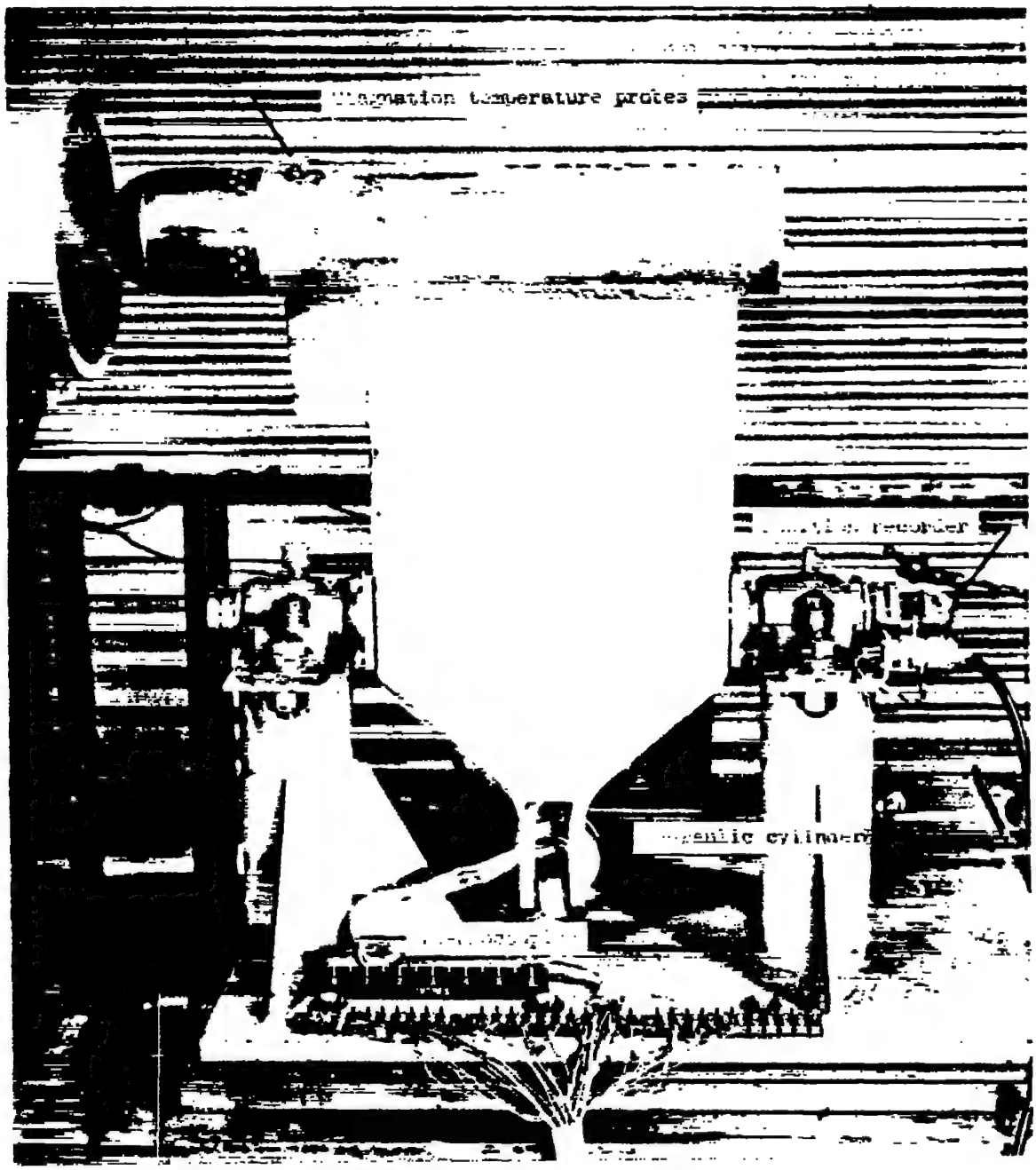

L-78137.1

Figure 1.- Photograph of 4-inch-diameter hemispherical nose mounted in the 8-inch auxiliary jet.

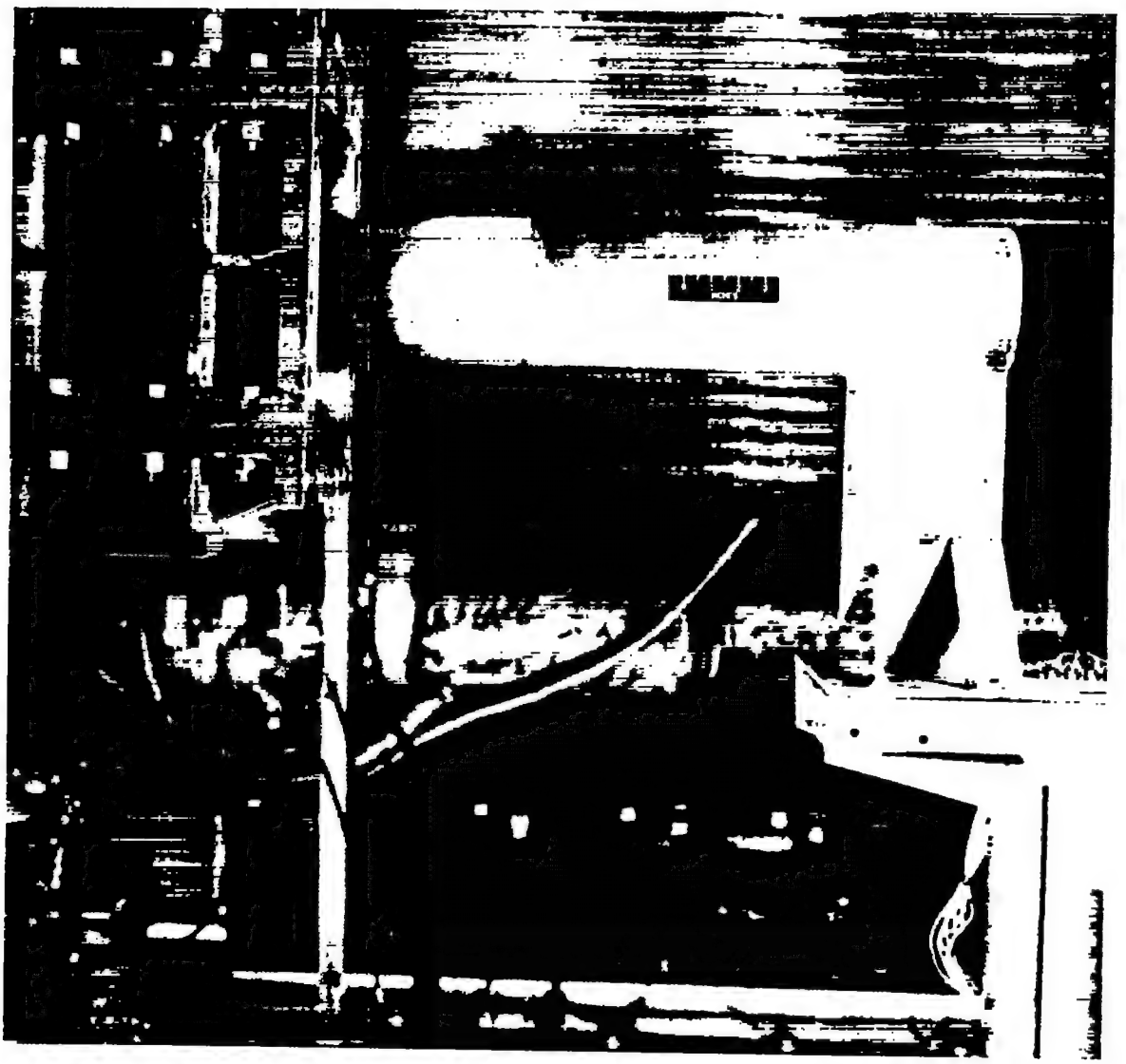

L-70981.1

Figure 2.- Photograph of the 6-inch-diameter hemispherical nose mounted in the main jet.

Symbol	Diam.	Mach number	Stagnation temperature	Surface condition
○	4 in.	1.62	820 °R	Smooth
□	4	2.05	997	
◇	4	2.54	1012	
△	4	3.04	980	
◺	6	1.99	986	Roughened
◺	6	1.99	967	Smooth

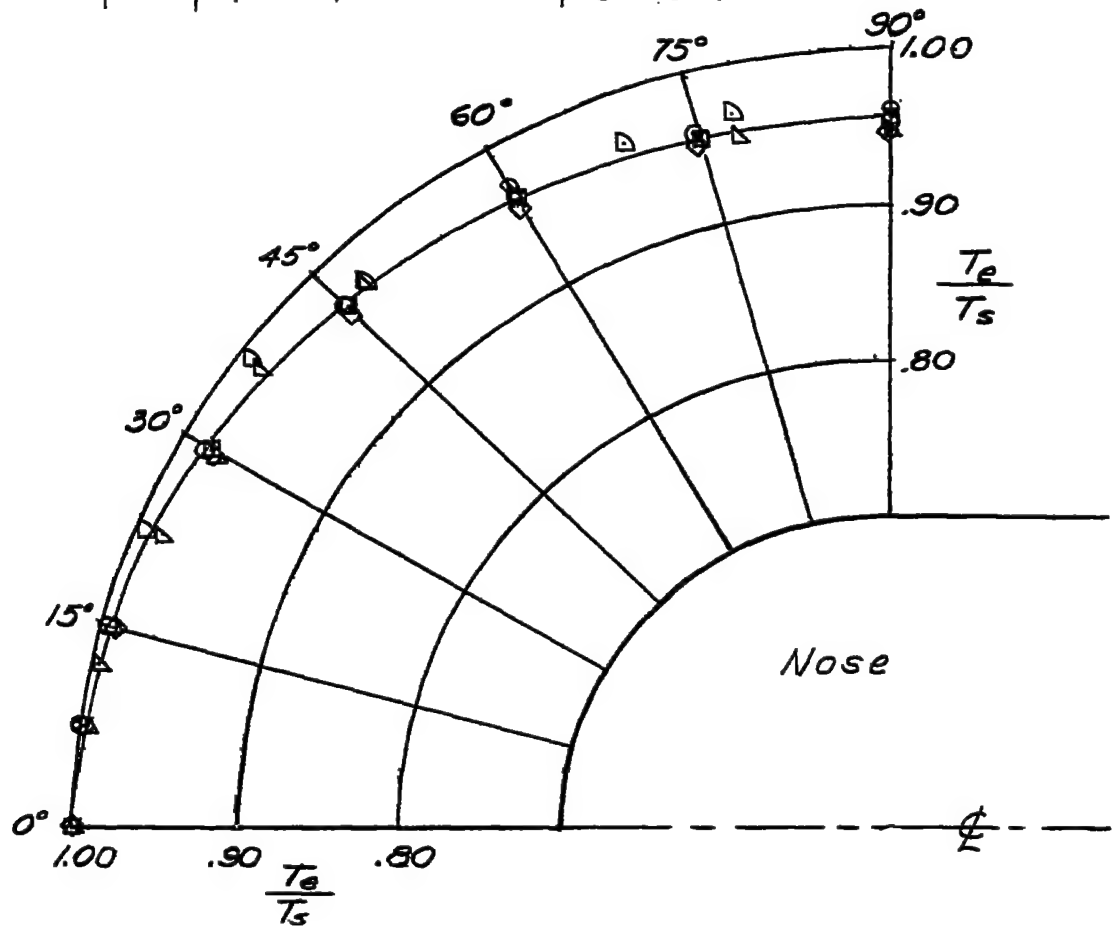

Figure 3.- Equilibrium skin temperature for the 4- and 6-inch-diameter hemispherical nose.

[redacted]

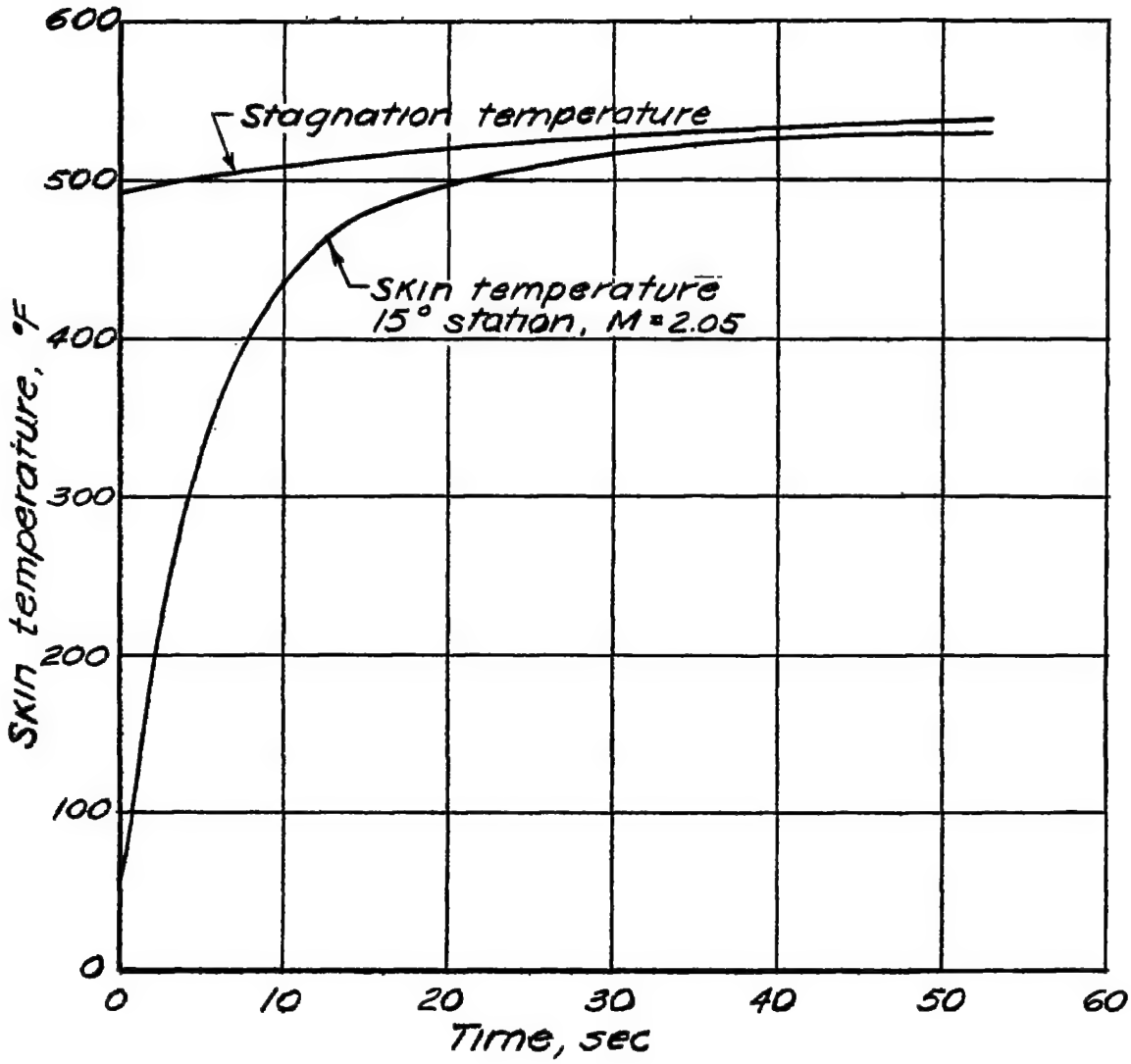

Figure 4.- Typical temperature-time histories.

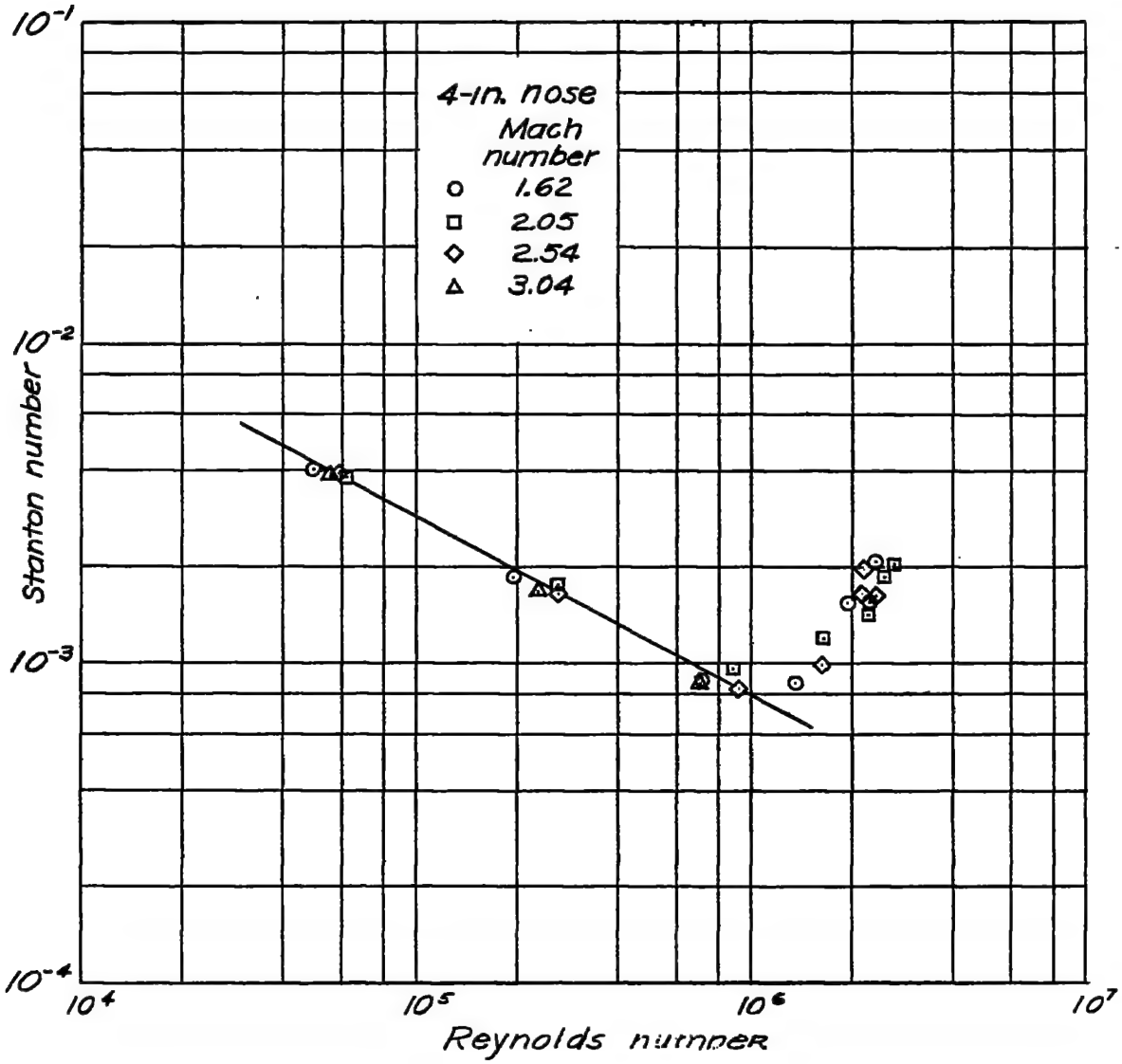

(a) $\frac{T_w}{T_{aw}} = 0.70$.

Figure 5.- Correlation of heat transfer for hemispheres with Reynolds number for various heating conditions.

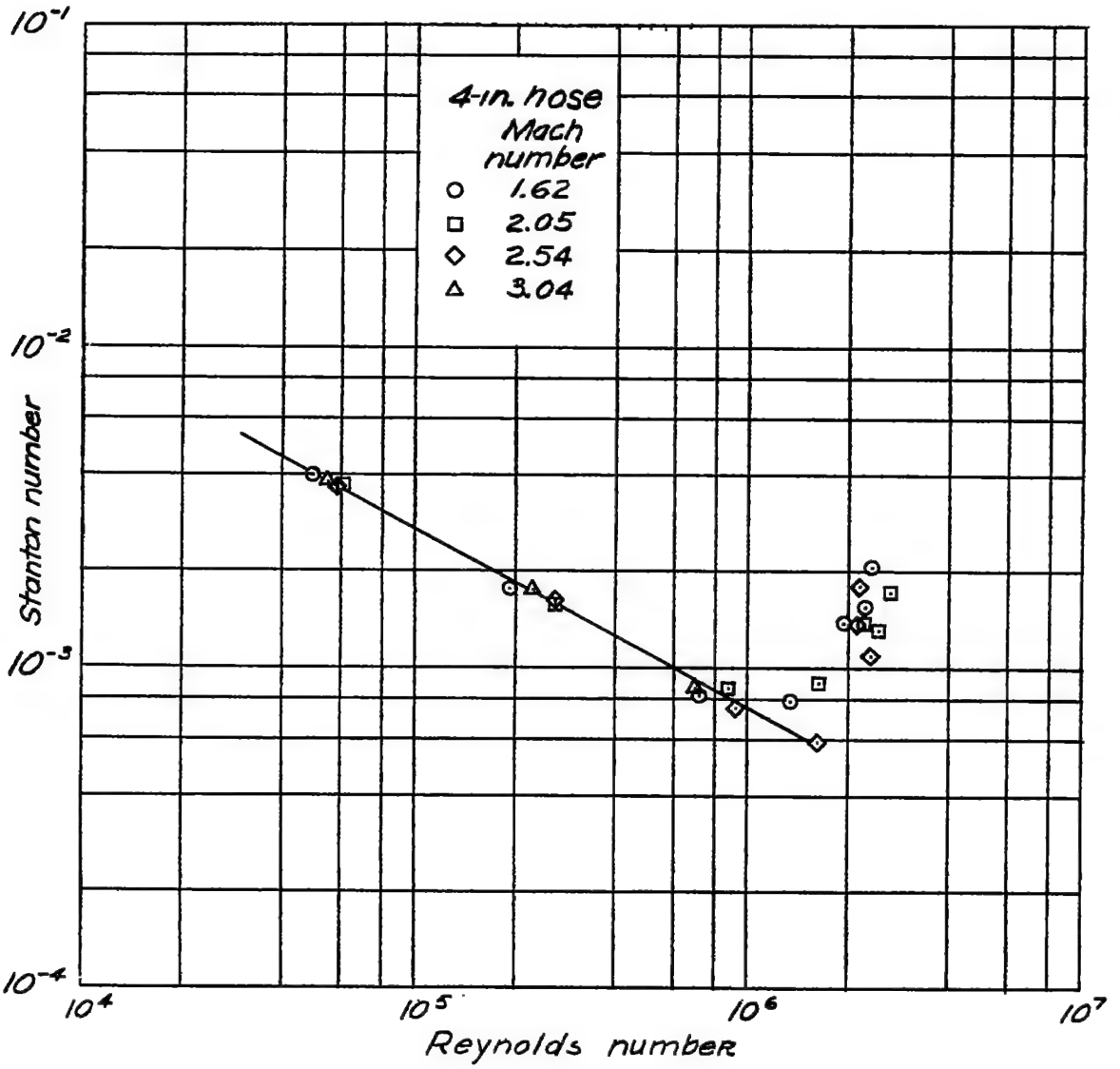

(b) $\frac{T_w}{T_{aw}} = 0.80$.

Figure 5.- Continued.

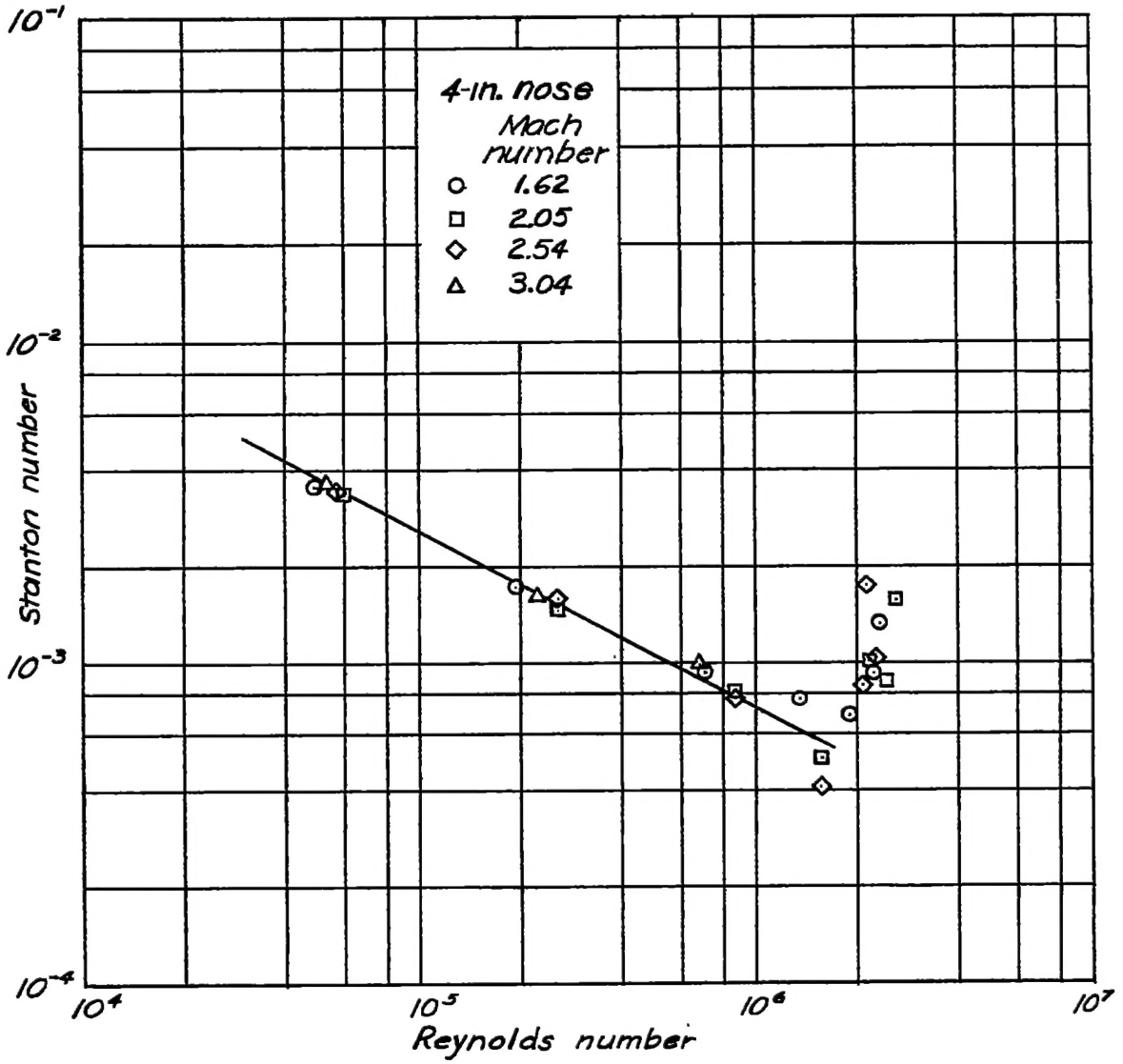

(c) $\frac{T_w}{T_{aw}} = 0.90$.

Figure 5.- Continued.

[redacted]

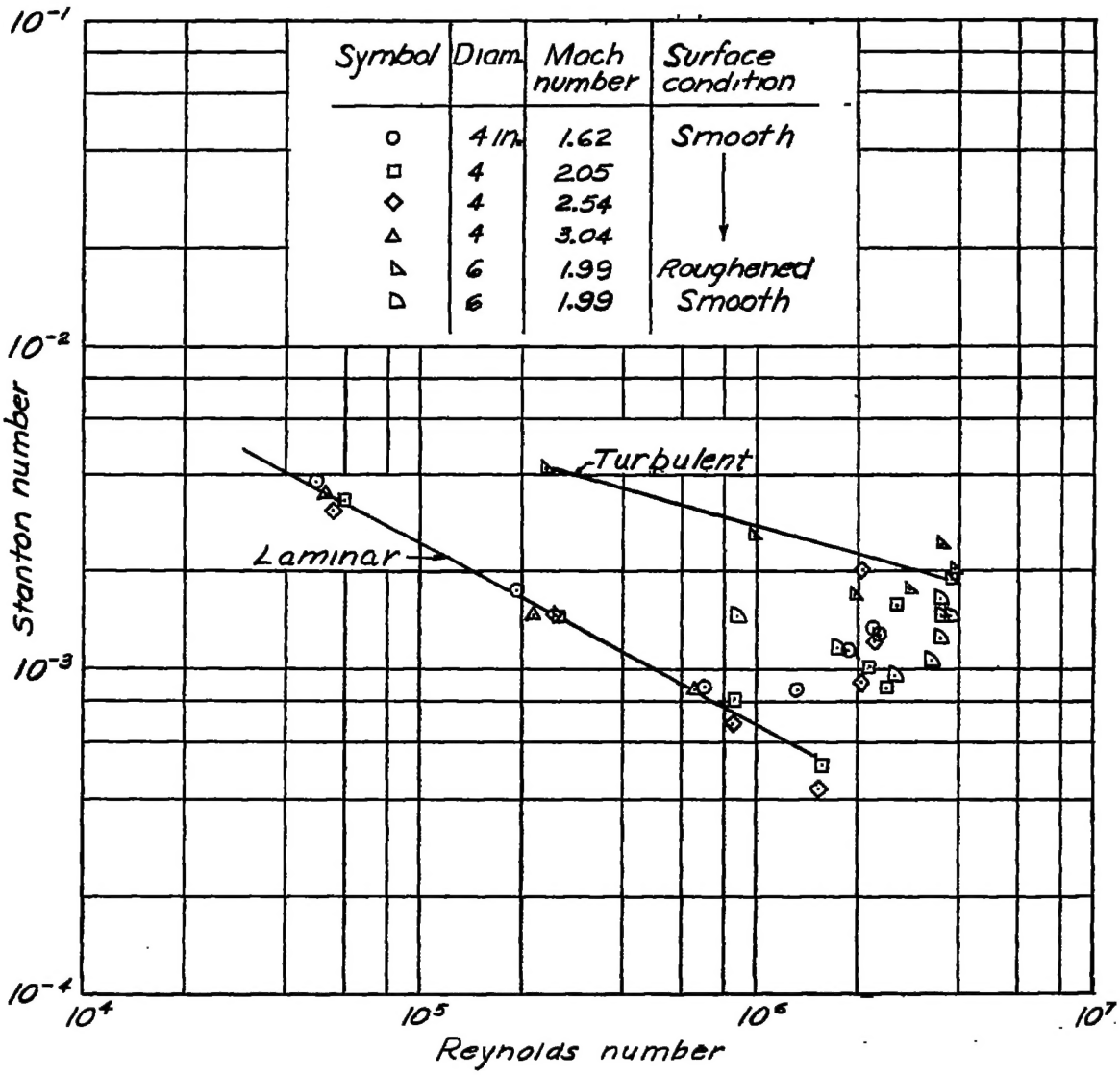

(d) $\frac{T_w}{T_{aw}} = 0.96.$

Figure 5.- Continued.

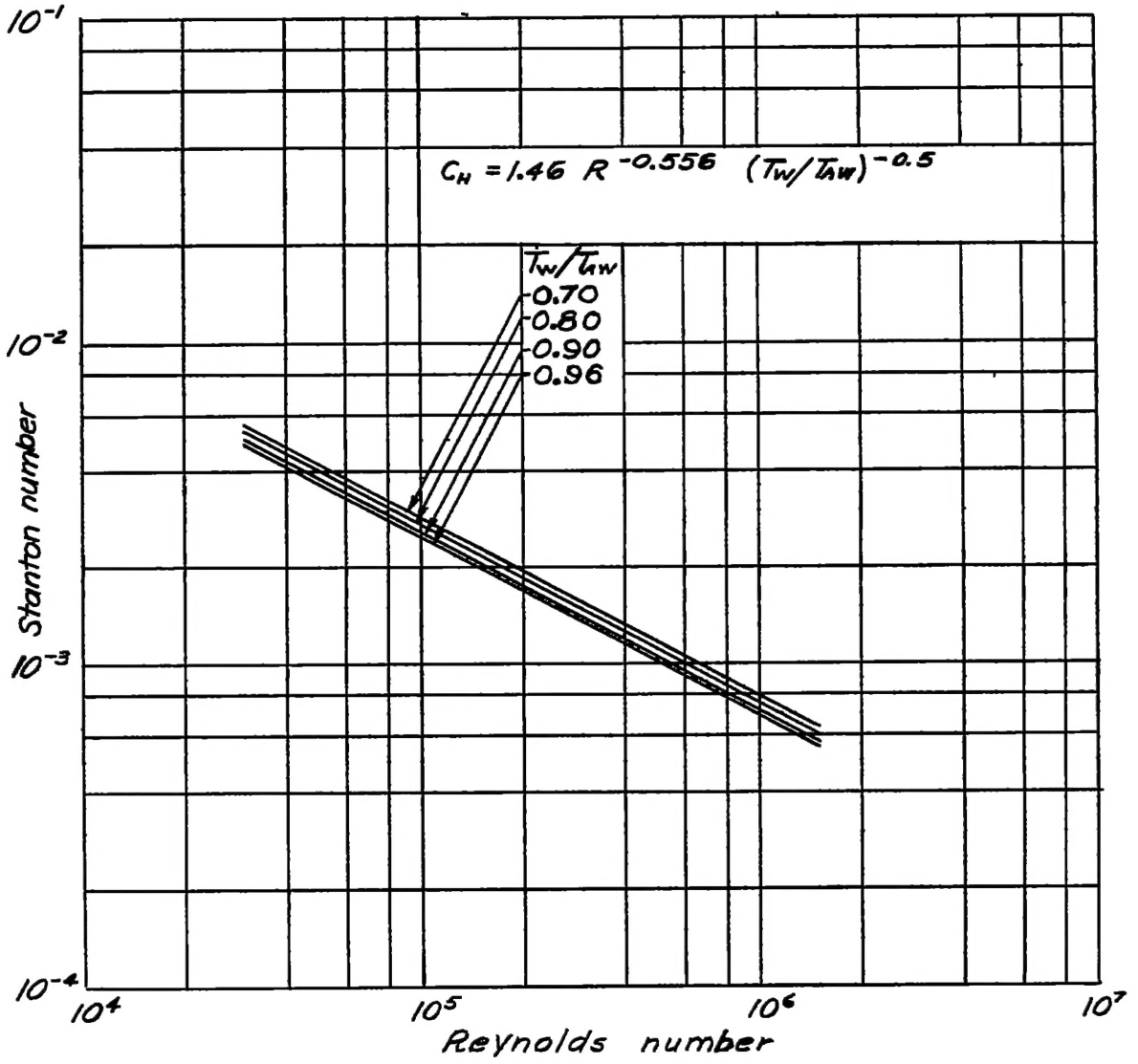

(e) Summary of the faired laminar heat-transfer data on hemispherical surfaces.

Figure 5.- Concluded.

[redacted]

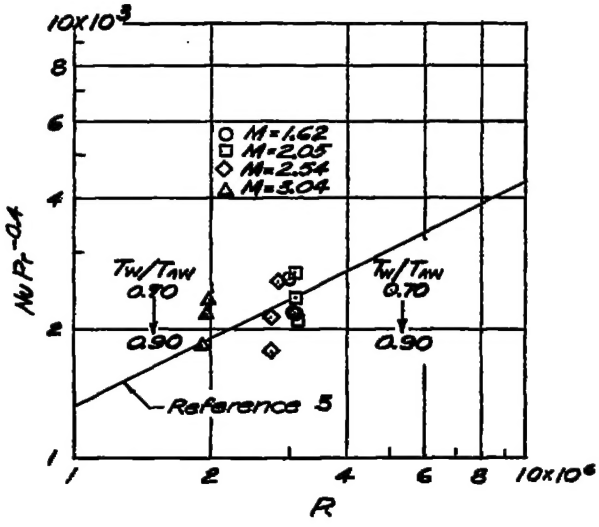

(a) Heat transfer.

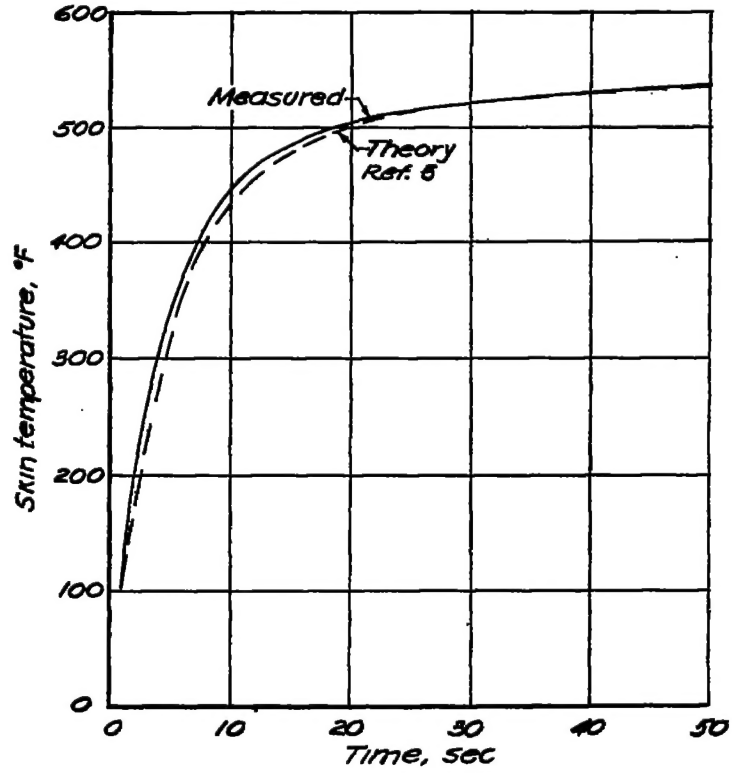

(b) Time history. M = 2.05.

Figure 6.- Comparison of measured and theoretical heat transfer at the stagnation point.

NACA-Langley - 2-3-54 - 325